# TECHNICAL RESEARCH REPORT


SYSTEMS RESEARCH CENTER

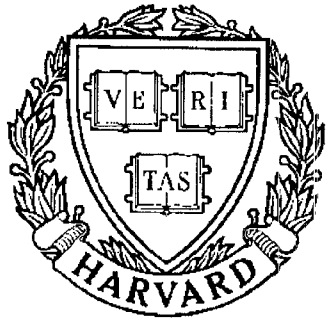


*Supported by the National Science Foundation Engineering Research Center Program (NSFD CD 8803012), the University of Maryland, Harvard University, and Industry*

# Bifurcation Analysis of Surge and Rotating Stall in Axial Flow Compressors

*by E.H. Abed, P.K. Houpt and W.M. Hosny*

TR 90-27r2

# Report Documentation Page

*Form Approved*
*OMB No. 0704-0188*



| 1. REPORT DATE | 2. REPORT TYPE | 3. DATES COVERED |
|---|---|---|
| **1990** | | **00-00-1990 to 00-00-1990** |

| 4. TITLE AND SUBTITLE | 5a. CONTRACT NUMBER |
|---|---|
| **bifurcation Analysis of Surge and Rotating Stall in Axial Flow Compressors** | 5b. GRANT NUMBER |
| | 5c. PROGRAM ELEMENT NUMBER |
| 6. AUTHOR(S) | 5d. PROJECT NUMBER |
| | 5e. TASK NUMBER |
| | 5f. WORK UNIT NUMBER |
| 7. PERFORMING ORGANIZATION NAME(S) AND ADDRESS(ES) **University of Maryland,Systems Research Center,College Park,MD,20742** | 8. PERFORMING ORGANIZATION REPORT NUMBER |
| 9. SPONSORING/MONITORING AGENCY NAME(S) AND ADDRESS(ES) | 10. SPONSOR/MONITOR'S ACRONYM(S) |
| | 11. SPONSOR/MONITOR'S REPORT NUMBER(S) |

12. DISTRIBUTION/AVAILABILITY STATEMENT
**Approved for public release; distribution unlimited**

13. SUPPLEMENTARY NOTES

14. ABSTRACT
**see report**

15. SUBJECT TERMS

| 16. SECURITY CLASSIFICATION OF: | | | 17. LIMITATION OF ABSTRACT | 18. NUMBER OF PAGES | 19a. NAME OF RESPONSIBLE PERSON |
|---|---|---|---|---|---|
| a. REPORT **unclassified** | b. ABSTRACT **unclassified** | c. THIS PAGE **unclassified** | | **21** | |

# Bifurcation Analysis of Surge and Rotating Stall in Axial Flow Compressors*

Eyad H. Abed†
Associate Professor
Department of Electrical Engineering
and the Systems Research Center
University of Maryland
College Park, MD 20742 USA

Paul K. Houpt
Manager, Industrial and Aerospace Controls
Control Technology Branch
Corporate Research and Development Center
General Electric Company
Schenectady, NY 12301 USA

Wishaa M. Hosny
Staff Engineer
Engine Operability Division
Aircraft Engines Business Group
General Electric Company
Cincinnati, Ohio 45215 USA

## ABSTRACT

The surge and rotating stall post-instability behaviors of axial flow compressors are investigated from a bifurcation-theoretic perspective. A sequence of local and global bifurcations of the nonlinear system dynamics is uncovered. This includes a previously unknown global bifurcation of a pair of large amplitude periodic solutions. Resulting from this bifurcation are a stable oscillation ("surge") and an unstable oscillation ("antisurge"). The latter oscillation is found to have a deciding significance regarding the particular post-instability behavior experienced by the compressor. These results are used to reconstruct Greitzer's (1976) findings regarding the manner in which post-instability behavior depends on system parameters. Moreover, the results provide significant new insight deemed valuable in the prediction, analysis and control of stall instabilities in gas turbine jet engines.

Manuscript: February 22, 1991

---

* Based on the paper: E.H. Abed, P.K. Houpt and W.M. Hosny, "Bifurcation analysis of surge and rotating stall in axial flow compressors," *Proceedings of the 1990 American Control Conference*, San Diego, pp. 2239-2246.

† Author to whom correspondence should be addressed.

# I. Introduction

A factor which severely limits the operating envelope of modern gas turbine jet engines is the fact that the axial flow compressor can become unstable when operated near its maximum achievable pressure rise. At such an operating condition, a moderate disturbance can result in instability, or even loss, of the nominal operating point. In this circumstance, the compression system can assume one of basically two types of dynamic behavior. The first, known as *surge*, is a large amplitude, periodic oscillation in which the compressor experiences a series of rapid flow reversals and recovery. The second, which is the more serious of the two, is known as *rotating stall* (or *nonrecoverable stall* ). This behavior is characterized by very inefficient engine operation at constant mass flow and pressure rise. A complete shutdown of the engine and subsequent re-start is usually required for recovery from this type of stall.

In this paper we investigate, from a bifurcation-theoretic perspective, the surge and rotating stall post-instability dynamic behaviors of axial flow compressors. A sequence of local and global bifurcations of the nonlinear system dynamics is uncovered. This is used to reconstruct Greitzer's [1] findings regarding the manner in which post-instability behavior depends on system parameters. Moreover, the results provide significant new insight deemed valuable in the prediction, analysis and control of stall instabilities in gas turbine jet engines.

Greitzer [1] introduced a lumped parameter, nonlinear model of axial flow compressor dynamics, simulations of which agreed with experimental results [2]. Among the key contributions of [1] was the introduction of a nondimensional parameter, $B$, whose value was found to be a determinant of the nature of post-instability compressor behavior (surge vs. rotating stall). Subsequently, others [7], [4] have sought to explain surge behavior by showing that Greitzer's model and extensions thereof support a Hopf bifurcation, i.e., the emergence of a periodic solution from an equilibrium point as a parameter is quasistatically varied. The main assumption in the Hopf Bifurcation Theorem is that a pair of eigenvalues of the system linearization cross the imaginary axis transversely at a critical value of the parameter (see, e.g., [3]).

In contrast, here we *do not* attribute surge in nonaxisymmetric axial flow compressors to this bifurcation. Rather, we present evidence for a bifurcation sequence which predicts the observations of Greitzer [1] for both surge and rotating stall. Hopf bifurcation, which has been noted by previous researchers, is accounted for in this work, but its role can be viewed is being of secondary significance. In this discussion, rotating stall and surge and their dependence on $B$ are considered from a global bifurcation standpoint. Special care is taken in the choice of an analytical model for the steady-state compressor characteristic which closely matches that reported by Greitzer [1]. Using this characteristic, we detect a global (so-called "cyclic fold") bifurcation of a pair of large amplitude periodic solutions. One of these is a stable limit cycle and corresponds to the surge type of stall, while the second is unstable and is therefore unobserved in experiments. We refer to this latter unstable oscillation as the *antisurge* oscillation, and to the former as

the *surge* limit cycle. We find that the changing size and shape of the antisurge oscillation determines the critical value of $B$ at which the post-instability behavior of the compression system switches from rotating stall to surge.

The presence of the global bifurcation of the surge and antisurge oscillations noted above depends strongly on the assumed compressor characteristic. For example, the cubic characteristic taken in [4] does not support such a bifurcation. We have chosen a more complicated algebraic model of the characteristic which faithfully represents *essential features* of the experimentally obtained characteristics studied by Greitzer [1],[2]. The critical values of $B$ reported here do not coincide exactly with those found in [1], but the reasons for this are apparent and further calculations, not reported in detail here, do result in agreement. Two main reasons for the apparent disagreement in critical $B$ values are our use of a reduced order version of the model employed in [1] and of an approximate analytic model of the compressor characteristic.

McCaughan [4] focused on an extension of Greitzer's model (Moore and Greitzer [5]) which reflects nonaxisymmetric flow dynamics in addition to the axisymmetric flow dynamics assumed in the model of [1]. In the present work, the *steady state* compressor characteristic, being based on the experimental characteristics reported in [1],[2], is nonaxisymmetric. However, nonaxisymmetric flow *dynamics* are not accounted for here, although the results of [5] can be used to extend the present work in that direction.

The paper is organized as follows. In Section II, we recall a nonlinear lumped parameter model from [1] for the dynamics of an axial flow compressor, and summarize the observations in [1] regarding dependence of the particular type of post-instability behavior on system parameters. In Section III, singular perturbation is used to reduce the order of the fourth order model of Section II, resulting in a second-order nonlinear model. The model used in our simulations for the steady-state compressor characteristic is also discussed in Section III. In Section IV, we present the bifurcation sequence which occurs as an important nondimensional parameter ($B$ [1]) is quasistatically varied. Analytical and simulation evidence for this bifurcation sequence, and implications for post-instability behavior, are also given in Section IV.

## II. Lumped Parameter Nonlinear Model

In this section, we recall the lumped parameter model of Greitzer [1] and summarize his observations regarding the circumstances of the appearance of the rotating stall and surge types of instabilities as a function of the nondimensional parameter $B$.

## II.1. The Model

The fourth order lumped parameter model introduced by Greitzer [1] is given, in nondimensional variables, by:

$$\frac{d\dot{m}_C}{dt} = B(C - \Delta P) \tag{1}$$

$$\frac{d\dot{m}_T}{dt} = (\frac{B}{G})(\Delta P - F) \tag{2}$$

$$\frac{d\Delta P}{dt} = (\frac{1}{B})(\dot{m}_c - \dot{m}_T) \tag{3}$$

$$\frac{dC}{dt} = (\frac{1}{\tau})(C_{ss} - C) \tag{4}$$

Here, $\dot{m}_c$ (resp. $\dot{m}_T$) is the nondimensional compressor (resp. throttle) mass flow, $\Delta P$ is the nondimensional plenum pressure rise, and $C$ is the nondimensional compressor pressure rise. The tilde notation used by Greitzer [1] for nondimensionalized quantities (e.g., $\tilde{\dot{m}}_C$, $\Delta\tilde{P}$) is not used here, due to the appearance here of only the nondimensional variables. Otherwise, the notation used above agrees with that of Greitzer. The steady state compressor pressure rise characteristic is denoted by $C_{ss}$ in (4), while $F$ denotes the throttle pressure drop characteristic (both nondimensionalized). Three parameters appear in Eqs. (1)-(4): $B$, $G$ and $\tau$. The first, $B$, is proportional to rotor speed. Expressions for the parameters $B$, $G$, and $\tau$ in terms of physical system parameters are given in [1]. Note that Eqs. (1)-(3) are based on physical considerations and a simplified system representation, while Eq. (4) is phenomenological and is meant to model the inherent relaxation of compressor pressure rise to the steady state characteristic. Hence, the value of the time constant $\tau$ is to be obtained experimentally.

The compressor and throttle characteristics $C_{ss}$ and $F$, respectively, are of fundamental importance in the analysis of system (1)-(4). This is because these characteristics are the source of the nonlinearity of Eqs. (1)-(4). The steady state compressor characteristic $C_{ss}$ (for an axial flow compressor) is often modeled as in Figure 1, in which a hysteresis loop appears. Note that for such a plot, the nondimensional plenum pressure rise $\Delta P$ is not a single-valued function of the axial velocity parameter $\dot{m}_c$. Note also that the plot contains two (hysteresis) branches which do not represent quasi-steady behavior, but rather indicate a "jump" (fast transient) between the lower and upper main branches of the characteristic. A quasi-steady characteristic may be obtained from that of Fig. 1 by replacing the two "jump branches" in the compressor characteristic with a single "transition branch" connecting the upper and lower branches of the characteristic, and smoothly connecting the remaining upper and lower branches of the characteristic. This is depicted in Figure 2 for the case in which the transition branch is positively sloped. With a positively sloped transition branch, the compressor characteristic is single-valued. Were the transition branch negatively sloped, the overall compressor characteristic would, at least for a range of values of mass flow rate, be triple-valued. Even a single-valued compressor characteristic such as that

depicted in Figure 2, however, can be consistent with the presence of a hysteresis loop. Hysteresis would occur as the throttle is slightly closed and then reopened.

To facilitate computer simulation of the model, we shall in the following adopt such a single-valued compressor characteristic. As for the throttle characteristic $F$, a typical plot also appears in Figure 1. Note that this is a single-valued function giving the throttle pressure drop $F$ in terms of the throttle mass flow $\dot{m}_T$. Moreover, the curve always has positive slope, and, for a variable area nozzle or valve type throttle, with ambient static pressure at the throttle discharge plane, we have the explicit representation

$$F = (\frac{A_c^2}{A_T^2})\dot{m}_T^2 \tag{5}$$

in terms of the flow-through compressor and throttle areas $A_c$ and $A_T$, respectively.

## II.2. Dynamic Behavior

Next we proceed to give a brief summary of the influence of the value of $B$ on the dynamic behavior of Eqs. (1)-(4), as discussed by Greitzer [1],[2]. All physical data used by Greitzer originated from an experimental three-stage axial compressor. For each case of interest, the model (1)-(4) was simulated and the results were compared with those obtained experimentally.

To understand the manner in which initial conditions for the simulation were set up, we first investigate the conditions for equilibrium operation of Eqs. (1)-(4). At an equilibrium point, we have

$$C = C_{ss} = \Delta P = F \tag{6}$$

and

$$\dot{m}_c = \dot{m}_T \tag{7}$$

Therefore, an equilibrium point of (1)-(4) occurs at the intersection of the compressor and throttle characteristics, graphed relative to the independent variable $\dot{m}_c$ (or, equivalently, $\dot{m}_T$). This is the same as saying that the steady state operating point is determined by the requirements that (i) the mass flow through the compressor and the throttle are the same, and (ii) the pressure rise through the compressor equals the pressure drop through the throttle. Figure 1 depicts this situation for a stable operating point near the peak of the steady state compressor characteristic.

Each simulation and corresponding experiment reported by Greitzer [1],[2] begins from an initial condition obtained by perturbing the throttle line slightly to the left of its position in Figure 1, with the operating point initially near the peak of the compressor characteristic. This is depicted in Figure 3. (Figure 4 depicts the effect of such a perturbation assuming a single-valued steady state compressor characteristic of the type shown in Figure 2.) Such a perturbation of

the throttle line may result, for instance, from slightly closing the throttle (cf. Eq. (5)). Depending on the values of system parameters, especially $B$, the system was then observed to either converge to the equilibrium point on the lower branch of the compressor characteristic (rotating stall), or to converge to a large amplitude periodic motion (surge). In Figures 3 and 4, the equilibrium on the lower branch of the compressor characteristic is denoted RSE, for *rotating stall equilibrium.*

The general dependence on $B$ of the mode of stall encountered is now reviewed. For each of the following cases, we are concerned mainly with the trajectory starting from the initial condition identified above, namely that at the peak of the compressor characteristic, with the throttle line perturbed slightly to the left of the peak of the compressor characteristic (as in Figures 3 and 4). The four cases are referred to as Regimes 1,2,3,4. Analytical and simulation evidence will be given in Section IV for these behaviors.

*Regime 1: Small $B$.* For small values of $B$, the trajectory settles on the rotating stall equilibrium. The motion is "over-damped," i.e., it doesn't exhibit an oscillatory component. (This is depicted in Fig. 5.)

*Regime 2: Moderate $B$.* At some point, although rotating stall is still the eventual limit of the trajectory, the transient is no longer over-damped, but is oscillatory.

*Regime 3: Large $B$.* For larger values of $B$, the trajectory no longer seeks the rotating stall equilibrium point, but rather converges to a large amplitude limit cycle motion. This is known as surge. (This is depicted in Fig. 6.)

*Regime 4: Very Large $B$.* As $B$ is increased further, the system still converges to a large amplitude, surge oscillation, but the nature and frequency of this limit cycle change drastically. Specifically, the limit cycle is now characterized by two time scales: a slow time scale while the trajectory remains near ("hugs") the compressor characteristic, and a fast time scale for motion between the main (left and right) compressor branches. (A figure illustrating this motion is given in Section IV.2.)

In the next section, the analytical model used in subsequent simulations is given. This involves order reduction of the model (1)-(4) as well as specification of the throttle and compressor characteristics.

## III. Second Order Nonlinear Model

In this section, the surge and rotating stall instabilities and their dependence on $B$ are obtained as by-products of a general nonlinear dynamic study of Eqs. (1)-(4). The first step is to re-draw the steady state compressor characteristic in a way which facilitates the analysis.

### III.1. Nonaxisymmetric Single-Valued Compressor Characteristic

As noted above, the hysteresis portion of the steady state compressor characteristic as it is typically drawn (see Fig. 1) contains a deficiency. Namely, it includes two branches which represent fast, *transient motions* as opposed to steady state behavior. Instead, we choose to employ a single-valued function as in Figure

2. The particular characteristic is presented in Section IV.2 below, which contains computer simulations illustrating the paper's main results.

## III.2. Second Order Reduced Model

The primary variables to the compressor user are mass flow ($\dot{m}_c$) and delivery pressure ($\Delta P$) [1]. It is possible to approximate the fourth order compressor model (1)-(4) by a second order model in these variables alone. Although this approximation is not necessary for the results given below, it is useful in simplifying computations. Two basic assumptions are needed to perform the model order reduction: first, that the relaxation to the steady state compressor characteristic implied by Eq. (4) occurs in a very short time (i.e., $\tau$ is small), and second, that the throttle inertial forces are negligible.

The first of these assumptions enables us to neglect Eq. (4) and replace $C$ in Eq. (1) by $C_{ss}$. This is easily justified using Tikhonov's Theorem from singular perturbation theory, since $\tau$ may be viewed as a singular perturbation parameter. The second assumption implies

$$\Delta P = F(\dot{m}_T), \tag{8a}$$

and hence that $\dot{m}_T$ is given by

$$\dot{m}_T = F^{-1}(\Delta P) \tag{8b}$$

These facts imply that the primary variables $\dot{m}_c$, $\Delta P$, are governed approximately by the system

$$\frac{d\dot{m}_c}{dt} = B(C_{ss}(\dot{m}_c) - \Delta P) \tag{9}$$

$$\frac{d\Delta P}{dt} = (\frac{1}{B})(\dot{m}_c - F^{-1}(\Delta P)) \tag{10}$$

For the quadratic throttle characteristic (5), the system (9), (10) takes the form

$$\frac{d\dot{m}_c}{dt} = B(C_{ss}(\dot{m}_c) - \Delta P) \tag{11}$$

$$\frac{d\Delta P}{dt} = (\frac{1}{B})(\dot{m}_c - \frac{A_T}{A_c}(\Delta P)^{1/2}) \tag{12}$$

Before investigating analytically the second order model (9), (10) (or (11), (12)), we should discuss the equilibrium points of the system. Consider either a hysteretic characteristic as in Fig. 1, or a single-valued characteristic as in Fig. 2. Depictions of an "equivalent" throttle line relating $\Delta P$ and $\dot{m}_c$ appear in Figs. 1 and 2, along with the compressor characteristic. Equilibrium points are given by the points of intersection of the compressor characteristic and the throttle line. If the throttle line is moved to the left (closing the throttle), the rotating stall equilibrium point appears, as shown in Figs. 3 and 4, respectively.

# IV. Bifurcations and Stall Phenomena

## IV.1. Local analysis at rotating stall equilibrium point

Denoting by superscript 0 an equilibrium value of a state variable, and by a prime differentiation with respect to the argument of a function, the Jacobian matrix of the second order reduced model (11), (12) is given by

$$B\begin{pmatrix} C'_{ss}(\dot{m}_C^0) & -1 \\ B^{-2} & -0.5A_T A_C^{-1} B^{-2}(\Delta P^0)^{-1/2} \end{pmatrix} \tag{13}$$

Singular perturbation results imply that as $B \to 0$ the eigenvalues of the Jacobian matrix are asymptotically given by

$$B(C'_{ss}(\dot{m}_c^0) - 2\frac{A_c}{A_T}(\Delta P^0)^{1/2}) + O(B^2), \tag{14a}$$

and

$$-\frac{A_T}{2A_c B(\Delta P^0)^{1/2}} + O(1). \tag{14b}$$

Each of the two quantities is both real and negative. (The former is negative because of the steepness of the throttle line, i.e., $A_c/A_T$ is large, and, concurrently, $C'_{ss}(\dot{m}^0)$ is relatively small.) The negativity of the eigenvalues for small $B$ is in agreement with the behavior discussed for Regime 1 in Section II.2 above, since it implies *overdamped* convergence of *nearby* trajectories to the equilibrium. Nothing can yet be said regarding the global behavior of trajectories.

As $B$ increases, the asymptotic formulae (14a), (14b) suggest that the eigenvalues approach one another, meet, and break off in conjugate directions into the complex plane. This can be checked with the aid of the characteristic polynomial of the Jacobian matrix (13). It is more convenient to work with the following polynomial, which is the characteristic polynomial of $1/B$ times the matrix of Eq. (13):

$$\lambda^2 + (\frac{A_T}{2A_c B^2(\Delta P^0)^{1/2}} - C'_{ss}(\dot{m}_c^0))\lambda + \frac{1}{B^2}(1 - \frac{A_T C'_{ss}(\dot{m}_c^0)}{2A_c(\Delta P)^{1/2}}) \tag{15}$$

The calculations are a bit involved.

The conditions for a Hopf bifurcation to occur for a given value of $B$ at a known equilibrium point are, from $C'_{ss}$, that

$$\frac{A_T}{2A_c B^2(\Delta P^0)^{1/2}} - C'_{ss}(\dot{m}_c^0) = 0, \text{ and} \tag{16a}$$

$$1 - \frac{A_T C'_{ss}(\dot{m}_c^0)}{2A_c(\Delta P)^{1/2}} > 0 \tag{16b}$$

Note that, since $C'_{ss}(\dot{m}_c^0)$ is negative at the original stable operating point (at the peak of the compressor characteristic), (16a) cannot be satisfied there. So a Hopf bifurcation cannot occur at that equilibrium. However, conditions (16a), (16b) can be satisfied at the rotating stall equilibrium point. Indeed, (16a) implies that the corresponding value of $B$ is

$$B^c_{\text{Hopf}} = \left(\frac{A_T}{2A_c(\Delta P^0)^{1/2}C'_{ss}(\dot{m}_c^0)}\right)^{1/2} \tag{17}$$

From (5) and (6) it follows, however, that

$$\begin{aligned} F'(\dot{m}_T^0) &= 2\left(\frac{A_c}{A_T}\right)^2 \dot{m}_T^0 \\ &= 2\frac{A_c}{A_T}(\Delta P^0)^{1/2} \end{aligned} \tag{18}$$

Together, (17) and (18) imply

$$B^c_{\text{Hopf}} = \frac{1}{(F'(\dot{m}_c^0)C'_{ss}(\dot{m}_c^0))^{1/2}}. \tag{19}$$

## IV.2. Bifurcation sequence and post-instability behavior

In this section, the facts discussed above are pieced together to yield an overall picture of the global dynamics of the system (1)-(4) as a function of the nondimensional parameter $B$. The transition from over-damped to under-damped convergence to the rotating stall equilibrium as $B$ is raised has already been explained. Also, we have seen that as $B$ is increased further, the rotating stall equilibrium undergoes a Hopf bifurcation and simultaneously loses its stability. The conclusions we reach in this section are based on a combined use of analysis and simulation. In the simulations, the steady-state compressor characteristic is modeled using a complicated algebraic formula which need not be reproduced here. It suffices to note that this formula achieves a characteristic curve which is a good approximation to that reported by Greitzer [1],[2] for a specific three-stage compressor.

We make some brief remarks on the simulations and the manner in which they are reported in the figures. The simulations were performed using the SIMNON software package. The figures illustrating simulation results also include the SIMNON commands used to generate the simulations. In the SIMNON code, $\dot{m}_c$ and $\Delta P$ were denoted by mcd and pd, respectively. The notation mcdr and pdr occurs in the commands in figures generated by simultaneous simulations in both forward and reverse time. These are the variables $\dot{m}_c$ and $\Delta P$, respectively, computed in reverse time.

Generally, for small values of $B$, if the throttle line is perturbed so as to intersect the compressor characteristic only at the rotating stall equilibrium, then the latter equilibrium is the *global attractor* for the system. That is, every initial

condition converges eventually to a rotating stall operating condition. Figure 7 depicts a simulation for the approximate model we used for $B = 0.15$. This figure illustrates the behavior just noted for small values of $B$. (This can be seen to hold under general conditions by using a Liapunov function argument applied to a one-dimensional reduced-order system obtained by viewing $B$ as a singular perturbation parameter. A simple quadratic Liapunov function in the (scalar) state variable of the reduced model can be seen to suffice.)

As $B$ is raised past a value $B_1$, *two initially identical periodic solutions are born, one stable and the other unstable,* and envelope the compressor characteristic. In the bifurcation literature, this is referred to alternatively as a cyclic fold bifurcation or a saddle-node bifurcation of periodic solutions. This is illustrated in Fig. 8, which depicts computer simulations of these periodic solutions for the hypothesized compressor characteristic. The unstable oscillation is found by simulation in *reverse time* with a judicious choice of initial conditions. Note that the unstable periodic solution lies within the stable one. We refer to the stable periodic solution as the *surge limit cycle* (or simply *surge*), and to the unstable periodic solution as the *antisurge oscillation* (or simply *antisurge*).

The antisurge oscillation forms the boundary of the domain of attraction of the rotating stall equilibrium point.[1] Note that, thus far, the peak of the compressor characteristic lies within the domain of attraction of the rotating stall equilibrium–agreeing with Greitzer's [1] simulation results (Regimes 1 and 2 of Section II.2 above). Thus, for these low values of $B$, rotating stall must prevail as the steady state post-instability behavior. In addition, the unstable periodic solution forms the finite part of the boundary of the domain of attraction of the companion stable periodic solution.

As $B$ is increased further, the amplitude of the antisurge oscillation decreases steadily, until past a value $B_2$, the nominal equilibrium at the peak of the compressor characteristic no longer lies within this periodic solution. Instead, it now lies within the domain of attraction of the stable periodic solution, and so is attracted to it. *This is the initiation of surge* (Regime 3 of Section II.2 above). Fig. 9 gives results of a simulation showing, in particular, the shrinking of the unstable periodic solution with increasing $B$. (In Fig. 9, $B = 0.45$.) Fig. 10 shows two simulations for the perturbed system, both starting at the same initial condition (the pre-stall equilibrium), but with slightly differing values of $B$. In one of the simulations, $B = 0.3757$, while in the other, $B = 0.3758$. For the smaller value of $B$, the rotating stall equilibrium is approached (trajectory (a) of Fig. 10). For the larger value of $B$, the surge oscillation is approached (trajectory (b) of Fig. 10). The simulation of Fig. 11 shows conclusively that this critical value of $B$, i.e., the value at which rotating stall gives way to surge, is precisely the value for which the antisurge oscillation passes through the initial condition.

As $B$ is increased still further, the surge oscillation continues to envelope

[1] This is true for the reduced second-order dynamic model. The implication for the full-order model is that the antisurge oscillation lies on the boundary of the domain of attraction.

the compressor characteristic. In contrast, the unstable periodic solution shrinks, becoming vanishingly small, and finally collapses onto the rotating stall equilibrium point at some value $B_3$. Indeed,

$$B_3 = B^c_{\text{Hopf}}$$

In Fig. 12, which corresponds to $B = 0.70$, the unstable periodic solution is shown by simulation to have reached a rather small amplitude. The Hopf bifurcation occurring in the model under consideration is simply this merging of the now small-amplitude antisurge oscillation with the rotating stall equilibrium point. For $B > B_3$, the rotating stall equilibrium point is no longer stable, and the unstable periodic solution no longer exists. The surge oscillation is now the global attractor of the system. Regime 3 of Section II.2 above is still in force.

We now proceed to prove the existence of this surge oscillation for very large $B$, and in doing so determine its location and character. For large $B$, the surge limit cycle is an instance of a *relaxation oscillation*, very much akin to the van der Pol oscillation. In this regime the oscillation is characterized by two widely separated time scales. This was observed by Greitzer [1], and was referred to as "Regime 4" in Section II.2 above. The situation is depicted in Fig. 13, which is purely illustrative. The proof below is closely related to a standard construction of the van der Pol oscillation. See for instance Nayfeh [6].

In the following, we admit any throttle characteristic $F$ with positive slope. Divide Eq. (9) by Eq. (10), to get

$$\epsilon \frac{d\dot{m}_C}{d\Delta P} = \frac{C_{ss}(\dot{m}_C) - \Delta P}{\dot{m}_C - F^{-1}(\Delta P)} \tag{20}$$

where $\epsilon := B^{-2}$. If $\epsilon = 0$, then

$$\Delta P = C_{ss}(\dot{m}_C),$$

which states that solutions are relegated to the steady state compressor characteristic. We shall assume that $\epsilon$ is very small, but nonzero. Referring to Figure 13, consider a solution curve that starts at point $Q$. Since $Q$ is off of the compressor characteristic, $d\dot{m}_C/d\Delta P$ is approximately $+\infty$ up to $Q_1$ where it hits the compressor characteristic. Since $d\dot{m}_C/d\Delta P$ is approximately $\pm\infty$ away from the compressor characteristic, the solution curve tends to stay on this characteristic. Also, from Eq. (10), and since point $Q_1$ lies to the right of the throttle line in Fig. 13, we will have that $d\Delta P/dt > 0$ while the solution remains near the right portion of the characteristic. This means that the trajectory will move away from $Q_1$ upward, until it reaches the vicinity of $Q_2$. There, the solution jumps horizontally to the left, since we will have $d\dot{m}_C/d\Delta P$ approximately $-\infty$. The solution then hits the compressor characteristic at $Q_3$ and again tends to remain on the characteristic. Since $Q_3$ lies to the left of the throttle line, Eq. (10) implies that $d\Delta P/dt < 0$ while the solution remains near the left portion of the characteristic. Hence the

solution moves downward along this branch, until it arrives at the vicinity of point $Q_4$. There, it makes a horizontal rightward jump to $Q_5$. The solution exhibits a periodic clockwise motion thereafter, following the upper and lower branches of the compressor characteristic, with the exception of the horizontal jumps from $Q_2$ to $Q_3$ and from $Q_4$ to $Q_5$.

## V. Conclusion

A bifurcation sequence which is useful in explaining the dependence of observed stall behavior of axial flow compressors on the nondimensional parameter $B$ has been presented. The presence of a previously unknown global bifurcation of a periodic solution pair has been detected and found to be of fundamental importance in predicting the nature of post-instability compression system behavior. Specifically, an unstable *antisurge* oscillation has been found to be present for a large range of values of the parameter, and the position of the initial condition relative to this oscillation was found to be the decisive factor in determining post-instability behavior.

Analysis of the limiting cases of the bifurcation sequence as well as computer simulation have been employed in verifying its validity. Further simulations, not reported here, indicate robustness of the conclusions to the compressor and throttle characteristics, within certain limits. Specifically, the results appear to hold for a large class of nonaxisymmetric compressor characteristics, but do not apply for axisymmetric models. They are thus expected to be useful in the analysis, interpretation of experimental data, and control design of axial flow compressors.

## Acknowledgment

The authors are grateful to C.N. Nett for helpful discussions. They also thank R. Chen, L.P. Harris, D.-C. Liaw, R. Mani, A. Spang and W.G. Steenken for many helpful comments. This work was supported in part by a contract to the University of Maryland from the General Electric Company, by NSF Grants ECS-86-57561 and CDR-88-03012, and by the AFOSR University Research Initiative Program under Grant AFOSR-90-0015.

## References

[1] E.M. Greitzer, "Surge and rotating stall in axial flow compressors: Part I—Theoretical compression system model," *ASME J. Engineering for Power*, Vol. 98, 1976, pp. 190-198.

[2] E.M. Greitzer, "Surge and rotating stall in axial flow compressors: Part II—Experimental results and comparison with theory," *ASME J. Engineering for Power*, Vol. 98, 1976, pp. 199-217.

[3] B.D. Hassard, N.D. Kazarinoff and Y.-H. Wan, *Theory and Applications of Hopf Bifurcation*, 1981, Cambridge, U.K.: Cambridge University Press.

[4] F.E. McCaughan, "Application of bifurcation theory to axial flow compressor instability," *ASME J. Turbomachinery*, Vol. 111, 1989, pp. 426-433.

[5] F.K. Moor and E.M. Greitzer, "A theory of post-stall transients in axial compression systems: Part I—Development of equations," *ASME J. Engineering for Gas Turbines and Power*, Vol. 108, 1986, pp. 68-76.

[6] A.H. Nayfeh, *Perturbation Methods*, 1973, New York: Wiley-Interscience.

[7] H. Razavi, *Nonlinear Global Stability Analysis of Compressor Stall Phenomena*, NASA CR-174908, 1985, Scientific Systems, Inc., Cambridge, MA.

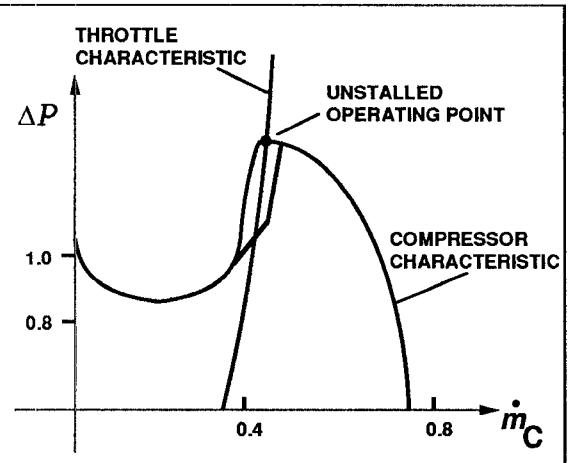


FIGURE 1. GENERIC COMPRESSOR AND THROTTLE CHARACTERISTICS

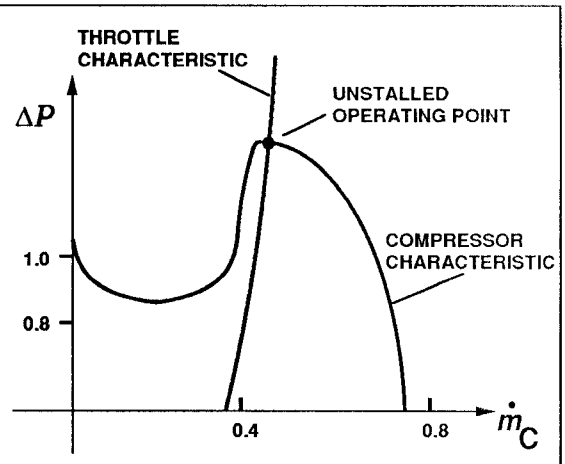


FIGURE 2. SINGLE-VALUED COMPRESSOR AND THROTTLE CHARACTERISTICS

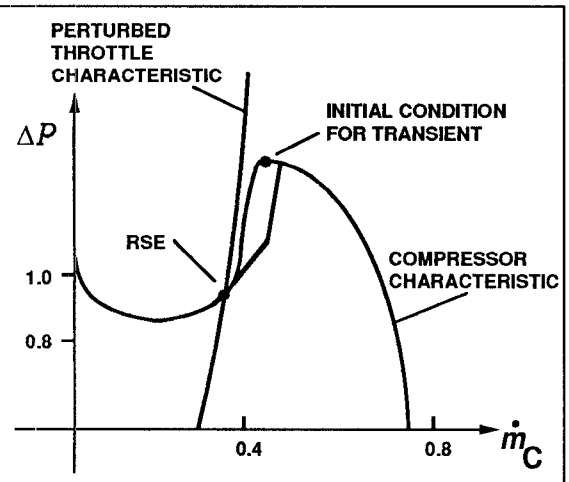


FIGURE 3. SHOWING EFFECT OF PERTURBED THROTTLE CHARACTERISTIC

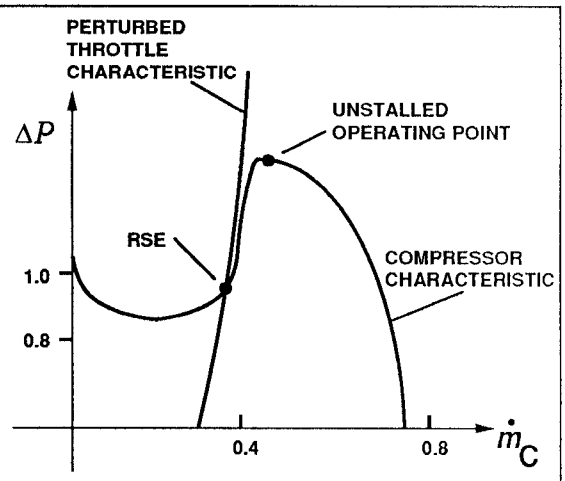


FIGURE 4. SHOWING EFFECT OF PERTRUBED THROTTLE CHARACTERISTIC

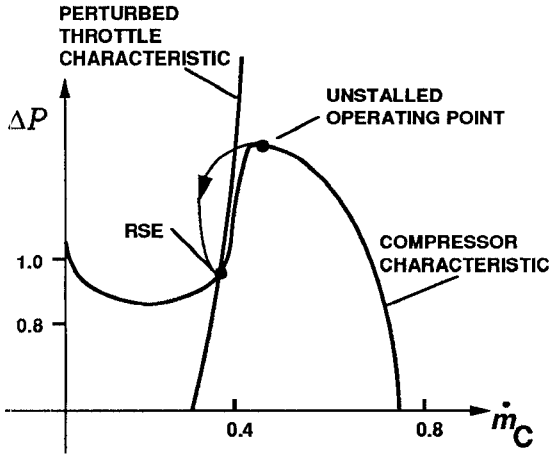


FIGURE 5. SHOWING OVERDAMPED CONVERGENCE TO ROTATING STALL

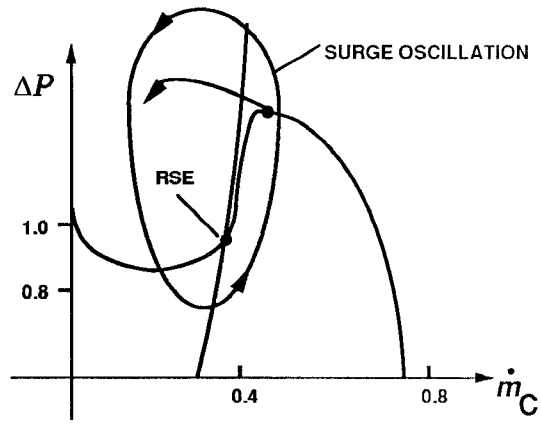


FIGURE 6. CONVERGENCE TO SURGE OSCILLATION

| SIMNON COMMANDS: | >init mcd:0.48 >init pd:1.22 >plot pd(mcd)<br>>par b:0.15 >simu 0 100 > |
|---|---|

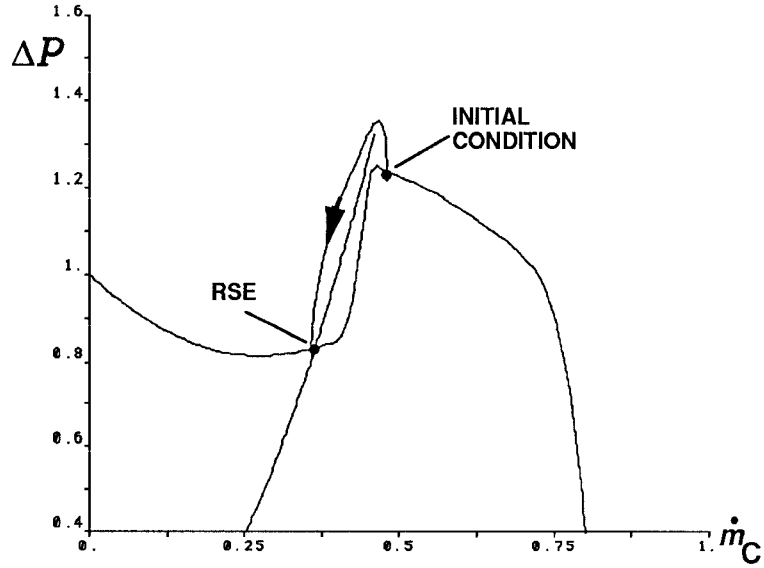


FIGURE 7. SIMULATION SHOWING CONVERGENCE TO ROTATING STALL ($B$ = 0.15)

| SIMNON COMMANDS: | >init mcd:0.24872 >init pd:0.72609 >plot pd(mcd)<br>>par b:0.368 >init mcdr :0.43213 >init pdr:0.9506<br>>simu 0 20 >plot pdr(mcdr) >simu > |
|---|---|

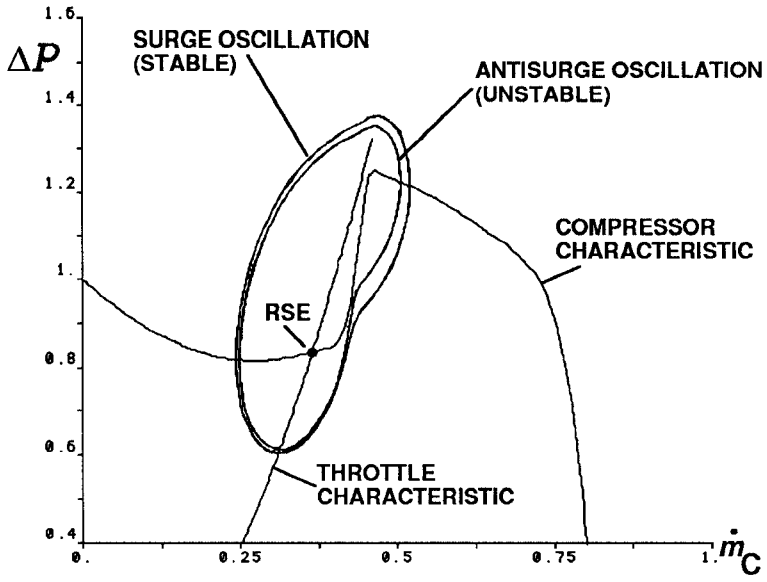


**FIGURE 8. SIMULATIONS SHOWING BIRTH OF SURGE AND ANTISURGE OSCILLATIONS ($B$ = 0.368)**

| SIMNON COMMANDS: | >init mcd:0.23425 >init pd:0.58022 >plot pd(mcd)<br>>par b:0.45 >init mcdr :0.30193 >init pdr:0.94693<br>>simu 0 20 >plot pdr(mcdr) >simu > |
|---|---|

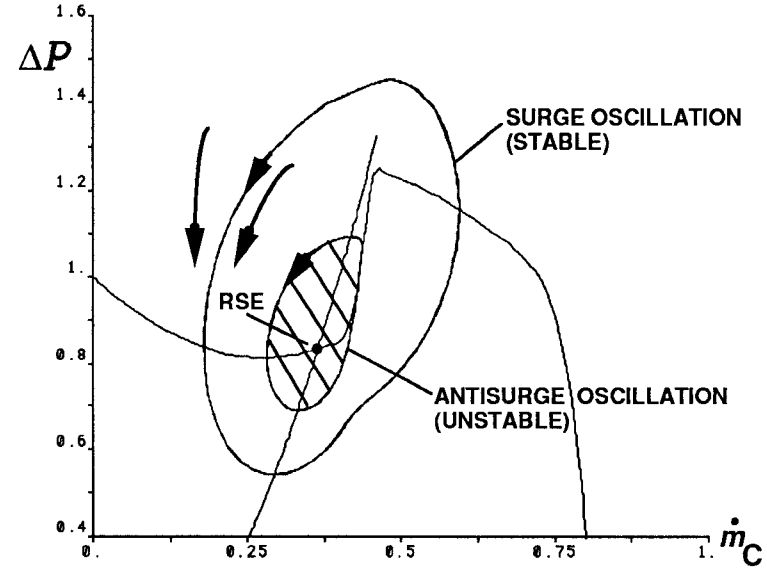


**FIGURE 9. SIMULATIONS SHOWING STABILITY DOMAINS AND OSCILLATIONS ($B$ = 0.45)**

| SIMNON COMMANDS: | >init mcd:0.48 >init pd:1.22 >plot pd(mcd)<br>>par b:0.3757 >simu 0 20 >par b:0.3758<br>>simu 0 10 > |
|---|---|

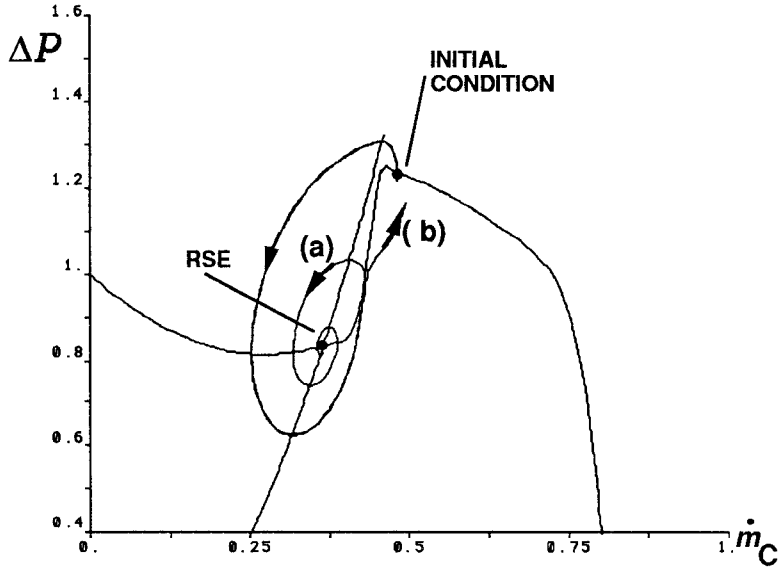


FIGURE 10. SIMULATION (a) YIELDS ROTATING STALL ($B$ = 0.3757); SIMULATION (b) YIELDS SURGE ($B$ = 0.3758)

| SIMNON COMMANDS: | >init mcd:0.48 >init pd:1.22 >plot pd(mcd)<br>>par b:0.3758 >simu 0 10 > init mcdr:0.48<br>>init pdr:1.22 >simu 0 20 > |
|---|---|

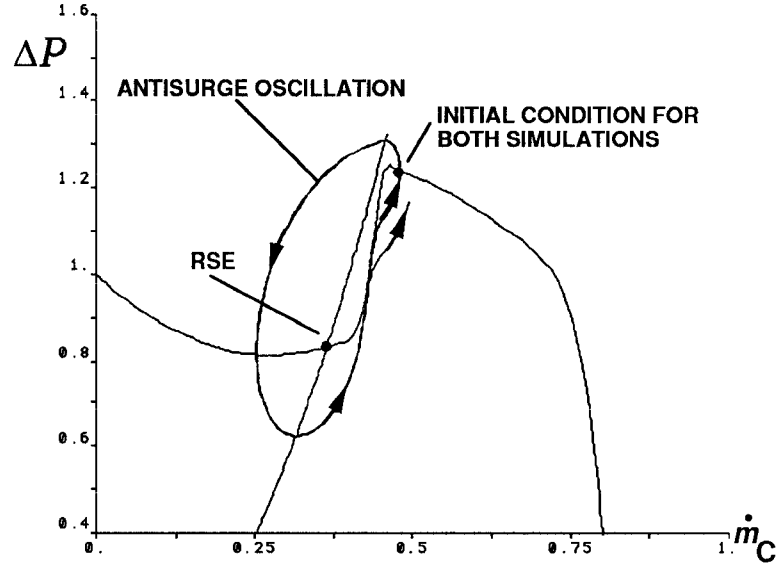


FIGURE 11. SIMULATIONS SHOWING COINCIDENCE OF SURGE INITIATION AND ANTISURGE OSCILLATION ($B$ = 0.3758)

| SIMNON COMMANDS: | >init mcd:0.31542 >init pd:0.53375 >plot pd(mcd)<br>>par b:0.70 >init mcdr :0.41029 >init pdr:0.85673<br>>simu 0 20 >plot pdr(mcdr) >simu > |
|---|---|

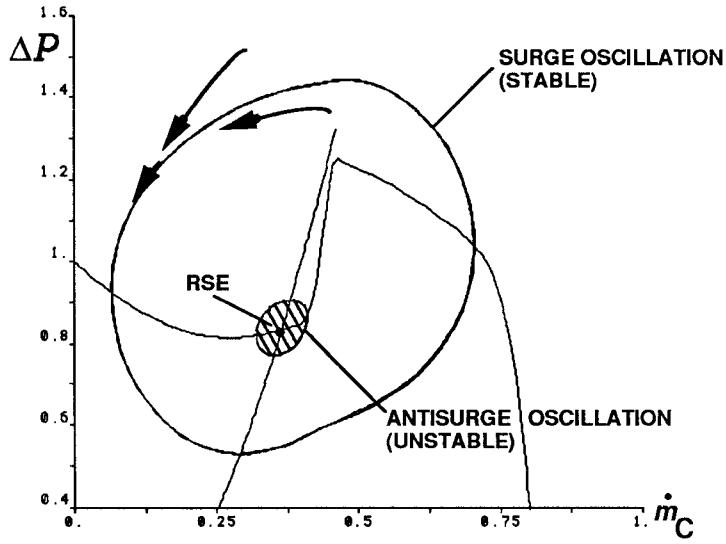


FIGURE 12. SIMULATIONS SHOWING SHRINKING ANTISURGE OSCILLATION ($B$ = 0.70)

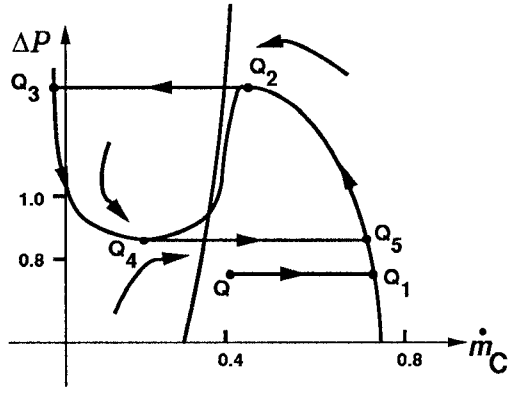


FIGURE 13. RELAXATION OSCILLATION FOR VERY LARGE $B$